Oxides Formed on Titanium by Polishing, Etching, Anodizing, or Thermal Oxidizing

J.R. Birch and T.D. Burleigh***

ABSTRACT

Photoelectrochemistry (PEC), glancing angle x-ray diffraction (GAXRD), electrochemical impedance spectroscopy (EIS), and potentiodynamic polarization (PDP) in synthetic salt water were utilized to investigate the nature of different oxides formed on titanium by thermal oxidizing, polishing, acid-etching, and anodizing. This work demonstrated that at least four different types of titanium oxide were formed on the surface of titanium, depending on the surface treatment. Rutile titanium dioxide (TiO_2) was formed on thermally oxidized titanium, and rutile provided the lowest passive current in seawater, the lowest bandgap (3.0 eV), and the highest photocurrent quantum efficiency of all the surface treatments tested. A titanium oxide-hydroxide with a bandgap of 3.5 eV was found on polished, acid-etched, or step-anodized (to 1.5 V) titanium. This same oxide-hydroxide was also present on the surface of cubic titanium monoxide (TiO) immersed in salt water. A second titanium oxide-hydroxide with a bandgap of 3.35 eV was found on the surface of slow ramp anodized titanium (to 2.0 V). Previous work by others has shown the presence of anatase on the surface of thick anodized titanium (bandgap of 3.2 eV).

KEY WORDS: anatase, electrochemical impedance spectroscopy, impedance, oxide, passivity, photoelectrochemistry, rutile, titanium

Submitted for publication June 1999; in revised form, August 2000.

* Materials Science and Engineering Department, 848 Benedum Hall, University of Pittsburgh, Pittsburgh, PA 15261. Present address: Allegheny Ludlum Corporation, Bagdad Plant, PO Box 565, Leechburg, PA 15656-1237.

** Materials Science and Engineering Department, 848 Benedum Hall, University of Pittsburgh, Pittsburgh, PA 15261. E-mail: burleigh@engrng.pitt.edu.

INTRODUCTION

The excellent corrosion resistance of titanium is a result of its ability to form a stable, protective, continuous, and adherent oxide film in the presence of air or water. Surface treatments such as thermal oxidation or anodizing can increase the thickness of the surface oxide and change its corrosion resistance. The surface treatment of the titanium also can affect the structure of this surface oxide. However, the structure of the surface oxide formed by different surface treatments is a matter of controversy.

The Pourbaix diagram illustrates that several forms of titanium oxide are possible at different pH and potentials, but titanium dioxide (TiO_2) was the only stable oxide within the stability limits of water.[1] The oxygen-titanium phase diagram indicates that many nonequilibrium forms of titanium oxide can exist.[2] Rutile is the most stable crystallographic phase of TiO_2, but lower temperatures favor the formation of metastable anatase over that of rutile.[2] Polymorphic transformations (anatase rutile and brookite rutile) can take place upon heating and are nonreversible. The crystallographic features of anatase and rutile are unique. The anatase structure has a higher degree of tetragonality than the rutile structure, and anatase is less closely packed. The tetragonal crystal structure of anatase has an a:c ratio = 1:1.8, where the unit cell dimensions are a = 5.36 Å and c = 9.53 Å. The density of anatase is 3.90 g/cm^3.[3] Rutile also has a tetragonal crystal structure but with an a:c ratio = 1:0.6, where a = 4.594 Å and c = 2.959 Å. The density of rutile is

0010-9312/00/000245/$5.00+$0.50/0

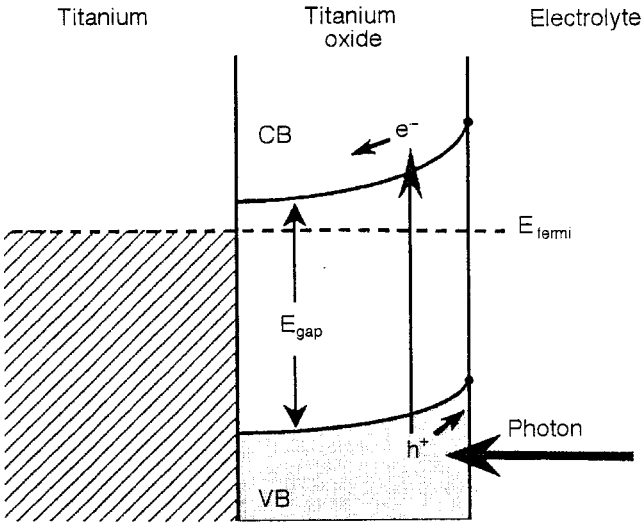

FIGURE 1. *The photocurrent is hypothesized to be generated by incident photons producing hole-electron pairs in the oxide. These hole-electron pairs are separated by the electric field and migrate to the opposite sides, creating the photocurrent.*

4.27 g/cm^3, ~ 9% denser than anatase.[3] The nature of these two oxides is clearly different.

To fully understand the corrosion behavior of titanium, it is important to understand the nature of the oxides that form on its surface. A freshly polished titanium surface will form an oxide film instantly when exposed to air or moisture. Andreeva, using ellipsometry, reported that the initial oxide film on titanium was ~ 1.4 nm in thickness, but grew to ~ 5 nm in 70 days, 8 nm to 9 nm after 545 days, and reached 25 nm after 4 years at room temperature.[4] Strongly oxidizing conditions such as thermal oxidation in air or anodizing in an electrolyte increase the oxidation potential of the surface. Tomashov reported that, at 800°C in oxygen and nitrogen, titanium formed an inner layer of titanium monoxide (TiO) and an outer layer of TiO_2 rutile (based on x-ray photography).[5] However, thermal oxidation at lower temperatures produced only TiO_2 rutile. Tomashov indicated that the anodic oxides, however, were either amorphous or microcrystalline anatase.[5] Leach and Sidgwick, using transmission electron microscopy and electron diffraction, reported that at low anodizing voltages the anodized layer had a glassy structure, and at higher voltages it became crystalline.[6] Blondeau, et al., reported that films anodized below 50 V were quasi-amorphous TiO_2, while films anodized above 50 V were a TiO_2 anatase modification, based on electron microscopy studies.[7] Yahalom and Zahavi postulated that below 5 V the titanium anodic oxides were amorphous, while above 85 V the anodic oxides were either anatase or amorphous, based on electron diffraction results.[8] McAleer and Peter reported that titanium anodic oxides grown to 40 V had a density similar to that of anatase, 3.9 g/cm^3.[9] Prusi and Arsov reported that electropolished titanium when analyzed with x-ray diffraction (XRD) demonstrated a rutile surface oxide.[10]

Thermal oxidation often is utilized to increase oxide thickness and corrosion resistance for extending service life. Schutz and Covington reported that the titanium oxide film formed by thermal oxidation has superior corrosion resistance over the oxide film formed by anodizing.[11] Anodically grown oxides can be removed by an acid pickle, but thermally grown oxides on titanium are much more resistant to an acid pickle, and their removal often requires sandblasting or a caustic descaling bath.[12] In boiling hydrochloric acid (HCl), the corrosion resistance of pickled and anodized specimens is poor compared to that of thermally oxidized specimens. The thermally oxidized tubes (677°C, 1 min) also showed significantly lower hydrogen uptake during cathodic charging than pickled or anodized titanium.[12]

Ohtsuka, et al., studied the anodic film on titanium using electrochemical impedance spectroscopy (EIS).[13] They reported that the anodic film was hydrated titanium oxide and may be represented by either $TiO_2(H_2O)_{1.4}$ or $TiO_{0.6}(OH)_{2.8}$.

Shibata and Zhu used transmission electron microscopy (TEM), Raman spectroscopy, and x-ray photospectroscopy (XPS) to study the anodic films on titanium.[14] They reported that the films formed at room temperature and at potentials < 5 V were usually amorphous. However, the film crystallized at temperatures > 60°C, or at potentials > 7 V, and formed microcrystalline anatase and rutile. The films contained much bound water, the percent depending on the formation conditions.

Pesant and Vennereau used photoelectrochemistry (PEC) and secondary ion mass spectroscopy (SIMS) to analyze the polished and the < 6-V anodic film on titanium.[15] They showed that the film was hydrated with many suboxides of titanium.

A method of evaluating the oxides on the titanium substrate is through the use of PEC.[16-30] Through PEC, the photospectra can be used to identify the oxide on the surface since the oxide has unique semiconducting properties such as its bandgap. The titanium oxides have been modeled as n-type semiconductors.[16-24] In this study, the metal/oxide interface was assumed to be an ohmic contact with no rectifying effects and minimal resistance. The oxide, however, was hypothesized to form an abrupt junction with the electrolyte, and the mismatch of the Fermi levels caused a space charge (represented by the band bending in Figure 1). Illumination of the oxide film with light with energy ($h\nu$) greater than or equal to the bandgap energy can excite electrons from the valence band to the conduction band. The band bending causes the excited electrons in the oxide conduction band to flow to the metal interface.

TABLE 1
Nominal Chemical Composition (wt%) of Grade 2 Titanium (UNS R50400)[A]

Iron	Oxygen	Carbon	Nitrogen	Hydrogen	Residuals (Each)	Residuals (Total)
0.12	0.10	0.10 max	0.03 max	0.015 max	0.1 max	0.4 max
0.30 max	0.25 max	—	—	—	—	—

[A] UNS numbers are listed in *Metals and Alloys in the Unified Numbering System*, published by the Society of Automotive Engineers (SAE) and cosponsored by ASTM.

There is also a flow of holes to the electrolyte interface that results in oxygen evolution (or dissolution) at the electrode surface. This photoinduced flow is the anodic photocurrent. By scanning the wavelength of light and recording the photocurrent, the quantum efficiency, Φ (with units of electrons/incident photon), of the oxide can be obtained. By plotting the square root of Φ vs photon energy, the indirect bandgap of the oxide can be extrapolated, which can be utilized to identify the oxide.

The following review illustrates the divergence in results and theories on the oxide films on titanium as measured by PEC. Koffyberg measured the quantum efficiency for photoelectrolysis of single crystal TiO_2 (reduced in hydrogen at 700°C for 8 h) and reported the first two indirect transitions to occur at 3.02 eV and 3.24 eV.[16] Schultze[17] and Leitner[18] measured the photoelectrochemical spectra on anodized titanium and reported an indirect bandgap of ~ 3.2 eV. Tyler utilized photoelectrochemical microscopy as a probe of localized properties of thin TiO_2 films.[19] For an oxide grown at 0.1 mV/s from –0.2 V to 2.7 V, the electron diffraction pattern had the rutile structure, as opposed to previously reported amorphous or microcrystalline anatase. Diffraction patterns from oxides grown at faster growth rates (1.0 mV/s) showed that the oxide film became more uniform and microcrystalline but that rutile was still the only phase found with electron diffraction.[19] In contrast, Shibata and Zhu used TEM and showed that the anodized titanium film formed at room temperature and 1.5 V was amorphous.[14] Burleigh measured the anodic oxide and single crystal TiO_2 rutile and reported that the anodic oxide formed by cyclic voltammetry (± 0.8 V) had a bandgap of 3.2 eV, while the single crystal TiO_2 had a bandgap 2.9 eV (Burleigh reported that this bandgap for rutile seems low).[20] Kozlowski, et al.,[21] continued the work of Tyler, et al.,[19] and also reported that the anodic oxides were rutile in structure (based on TEM). Kozlowski, et al., reported the indirect gap for slow grown (0.1 mV/s) anodic oxides to be 3.3 eV, and rapid grown anodic oxides to be 3.4 eV, in contrast to the reported indirect gaps for rutile as 3.0 eV and anatase 3.2 eV.[21] They explained the discrepancy in the bandgap measurement as caused by the variations in substrate structure and preparation, stating that large grain polycrystalline substrates may have produced oxides different from those formed on thin foil consisting of small, mechanically deformed crystals. Halley, et al.,[22] continued the research of Tyler, et al.,[19] and Kozlowski, et al.,[21] showing that the anodic oxide photospectra matched the photospectra from Koffyberg's[16] single crystal rutile, thus showing that the anodic oxide was TiO_2 rutile. Makuta, et al., tested titanium chemically reacted and thermally oxidized with PEC and reported a rutile surface with an indirect bandgap of 3.02 eV.[23] They reported that oxide formed by chemical reaction only was amorphous TiO_2 with an indirect bandgap of 3.35 eV. Kavan, et al., used PEC and reported that the indirect bandgap of single crystal anatase was 3.2 eV and single crystal rutile was 3.0 eV.[24] Marsh and Gorse used EIS and PEC to study anodically formed titanium films.[25] They reported that PEC showed modifications of the anodic film over the whole range of potential maxima, including a sub-bandgap contribution. Other authors have reported on the effect of growth rate on the anodic oxide on titanium.[30-32]

The variety of oxides and bandgaps in the above literature has sparked this present investigation into the photoelectrochemical analysis of the oxides formed on titanium. Most authors agree that the indirect bandgap for rutile is 3.0 eV and that for anatase is 3.2 eV. Yet there is disagreement on what oxide is present on the surface of titanium for the different surface treatments.

EXPERIMENTAL PROCEDURES

The titanium metal utilized in these experiments was commercial Grade 2 titanium in the form of tubing and flat sheet. The nominal composition is shown in Table 1. This titanium was cut into squares of 1 cm^2 or 1 $in.^2$ for the different tests. The initial surface treatment prior to all experiments was to wet-polish with 600-grit silicon carbide (SiC) in distilled water. Each specimen was then ultrasonically cleaned in acetone (CH_3COCH_3), dried, and then rinsed once again in distilled water.

The different surface treatments are listed in Table 2. They consisted of the wet, polished surface (with two different degrees of roughness), an acid

TABLE 2
Surface Treatments for the Titanium

600-grit SiC paper wet polish.
1-μm-grit alumina slurry wet polish.
Thermal oxidation ranging from 500°C to 800°C for 10, 30, and 60 min.
Pickling (acid etching) in HF-HNO_3 solution (Table 3).
Anodizing at various voltages at different ramping rates (Table 4).

TABLE 3
Pickling Solution

Volume (%)	Electrolyte
5	HF (48% concentration)
45	HNO_3 (65% concentration)
50	H_2O

etch (pickled), thermally oxidized in air, and anodized in 1 N sulfuric acid (H_2SO_4). The pickling solution is shown in Table 3. Samples were immersed in the solution for 3 min to 4 min and immediately rinsed with distilled water to prevent discoloration. The titanium was anodized with a potentiostat in 1 N H_2SO_4 to the given voltages and at the ramping rates shown in Table 4. After ramping, they were held at the final voltage for 10 min to reach steady state. Thermal oxidation was carried out in a furnace with an air atmosphere at 500, 600, 700, and 800°C for times of 10, 30, and 60 min. The colors of the thermally oxidized surfaces varied from clear, to straw yellow, to blue, to violet, and to dark metallic gray for the different temperatures and times. After the specimens were removed from the furnace, they were allowed to cool at room temperature.

The rutile TiO_2 single crystals had <001> orientation. High-purity powders of TiO_2 rutile (99.5%), TiO_2 anatase (99.9%), cubic TiO (99.9%), and Ti_2O_3 (99.8%) were mixed with epoxy and then pressed into wafers and allowed to cure. The epoxy was Devcon Corporation† 2-ton clear 2-part epoxy, which was more water resistant than the 5-min epoxy. The cured wafers were ground on 600-grit paper until paper thin, and an ohmic contact was made on the back of the sample by rubbing on a gallium-indium eutectic alloy. This was the same ohmic contact that was made on the single crystal TiO_2 rutile specimens. The gallium-indium contact then was connected to a copper wire with silver conducting paint and allowed to dry. Specimens were encased next in the epoxy (except for a small window on the front surface), allowed to cure, and tested with PEC. This epoxy-powder technique was found to be partially successful and was based on a powder sintering and vacuum epoxy casting of Schmüki, et al.[33]

After the surface treatment to form the oxide, the titanium samples were prepared for the different tests. Samples for PEC were electrically connected on the back surface to a copper wire, and then the entire sample was coated with the epoxy, except for a small window (~ 0.3 cm^2) on the front surface where the incident light was focused. For the EIS and potentiodynamic polarization (PDP) tests, a neoprene O-ring (2 cm inside diameter), thinly coated with Apiezon L† vacuum grease, was pressed against the titanium surface and then connected to the corrosion cell with a glass seal. (The vacuum grease prevented crevice corrosion under the O-ring, but was otherwise inactive.) The exposed sample surface area was 2.5 cm^2. The PEC and EIS measurements were made by polarizing the sample at its open-circuit potential.

The PEC test equipment was similar to that described previously.[20] A 150-W xenon arc lamp was the light source. The light was chopped into 13.8-Hz pulses by a rotating blade in an EG&G model 125A† chopper. A McPherson GM252† monochromator was used to select the desired wavelength of light typically between 200 nm and 420 nm. The corrosion test cell was enclosed in an aluminum Faraday cage. The light entered the corrosion cell through a Suprasil 2† fused quartz window. The voltage and current were monitored with a potentiostat using the three-electrode method. A lock-in amplifier was used to measure the magnitude of the photocurrent or impedance. The electrolyte in all experiments was synthetic seawater, meeting ASTM[1] D1141-52 standards. The EIS spectra were measured at the open-circuit potential using a 5-mV (rms) signal and a surface area of 2.5 cm^2. The PDP was measured in quiescent synthetic seawater at a ramp rate of 10 mV/s, starting at -500 mV vs silver-silver chloride (Ag-AgCl). The PEC signal was measured with the lock-in amplifier, which measured the magnitude

† Trade name.
[1] ASTM, 100 Barr Harbor Dr., West Conshohocken, PA 19428.

TABLE 4
Anodizing Conditions

Applied Voltage (V_{SCE})	Slow Ramping Rate (0.1 mV/s)	Medium Ramping Rate (1 mV/s)	Step Ramping (Single Step)
0.5		X	X
1.0	X	X	X
1.5		X	X
2.0		X	X

of the photocurrent at 13.8 Hz, and the photocurrent was recorded on the X-Y plotter.

Photospectra were measured at the open-circuit potential and are reported in terms of quantum efficiency (Φ), which has the units of electrons per incident photon. If each incident photon causes one measurable electron, then Φ = 1. The Φ was calculated at each wavelength by the following equation (derived by Burleigh):

$$\Phi = \frac{1.24 \times i_{photo}}{P_{lamp} \times \lambda} \quad (1)$$

where i_{photo} is the photocurrent (nA/cm²) at wavelength λ, P_{lamp} is the power (μW/cm²) of the monochromatic light from the arc lamp at wavelength λ, and λ is the wavelength (nm) of the incident light. The photocurrent was determined from the settings of the lock-in amplifier and potentiostat. The area was either the surface area of the sample or the area illuminated by the light (0.3 cm²), whichever was smaller. The λ was read directly from the monochromator dial. P_{lamp} was the more difficult quantity to determine. The power output was determined at each λ with a calibrated silicon photodiode (EG&G Judson model HUV-2000B[†]). This silicon photodiode was placed inside the corrosion cell (which was filled with distilled water) at the exact location of the PEC samples. The power of the monochromatic light was measured after the light had passed through the monochromator, through the fused quartz window, and through 2 cm of distilled water. The measured value was then corrected based on the calibration curve for the photodiode and by the power of the monochromatic light as measured at visible frequencies. As a result of the difficulty in determining the power output of the light, Φ is taken as an approximation and not as an absolute value.

For the EIS test, the oxide film can be approximated as a parallel plate capacitor at frequencies where the phase angle approaches -90°. With the above approximation, the following equation can be utilized to determine the thickness of the oxide layer:[34]

$$d = \varepsilon_1 \varepsilon_0 A 2\pi f (Z - Z_0) \quad (2)$$

where d is the thickness of the layer, ε_1 is the dielectric constant of TiO_2 (110 for rutile and 48 for anatase, according to Clark[3]), $\varepsilon_0 = 8.854 \times 10^{-12}$ F/m (dielectric of free space), A is surface area (~ 2.5 cm²), f is the frequency (Hz), Z is impedance (Ω) at frequency f, and Z_0 is impedance at high frequency (solution resistance). Since the oxide thicknesses were all in the submicron range, the effect of the depletion zone (normally on the order of microns) was not considered.

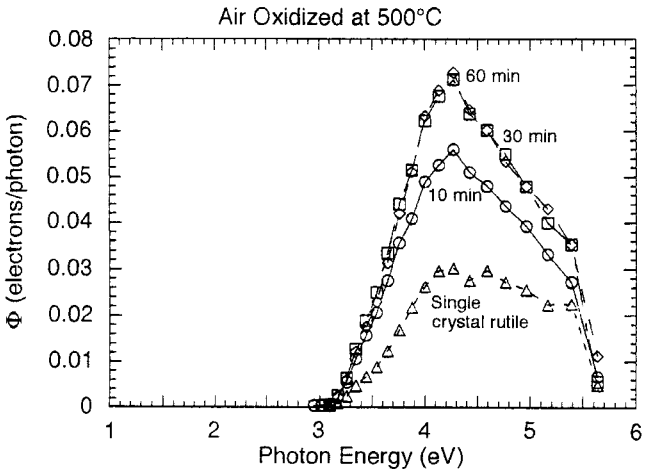

FIGURE 2. *The photospectra for oxidized titanium heated at 500°C for 10, 30, and 60 min are compared to the photospectra for single crystal rutile.*

Glancing angle x-ray diffraction (GAXRD), also known as parallel beam XRD or as thin film XRD, is a technique used to characterize thin surface films. The procedure only samples the top 100 nm of the surface. Diffraction lines may be utilized to determine the crystallographic spacing of the planes, which can be used to determine the composition and crystal form, using the standard diffraction data from the Joint Committee on Powder Diffraction Standards (JCPDS).[35] GAXRD tests were conducted on a parallel beam system with a 1.0° incident x-ray beam.

RESULTS AND DISCUSSION

The oxide layer formed on titanium was a function of the surface treatment experienced by that sample. The different photospectra resulting from the different surface treatments are shown herein and are compared to the photospectrum of single crystal rutile <001> orientation.

Figure 2 shows the PEC spectra for the titanium air oxidized at 500°C for 10, 30, and 60 min. Overlaid is the spectrum for the single crystal TiO_2 rutile. The maximum photocurrent/photon (Φ) for the 60-min oxide occurred at 4.3 eV (290 nm), when seven electrons were emitted per 100 incident photons (7% quantum efficiency or yield). Figure 3 has the same data as Figure 2, but replotted for the normalized square root of Φ. The linear portion of the curve was extrapolated to the x-axis to determine the bandgap of the surface oxide. All four of these samples exhibited the same bandgap of 3.0 eV, which corresponds to TiO_2 rutile. (This result agrees with the x-ray work of Tomashov.[5]) Figure 4 shows the normalized square root of Φ for the 600-grit polished titanium, the step anodized (1.5 V) titanium, and the crystal of cubic TiO. These three samples all exhib-

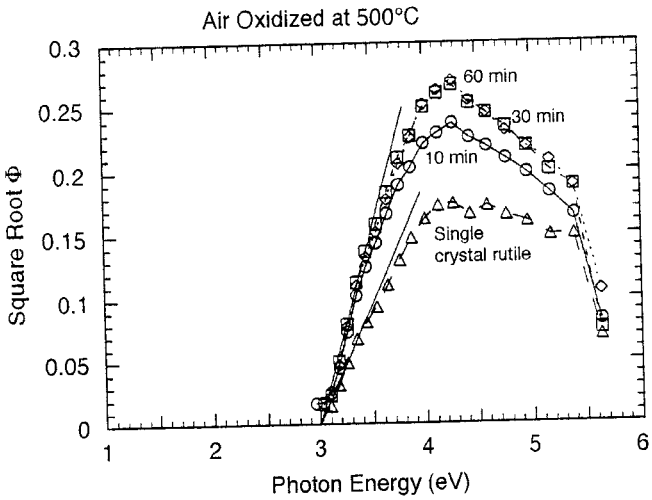

FIGURE 3. *The thermal oxide, single crystal rutile, and powder rutile (not shown) all demonstrate an extrapolated indirect bandgap E_{gap} = 3.0 eV.*

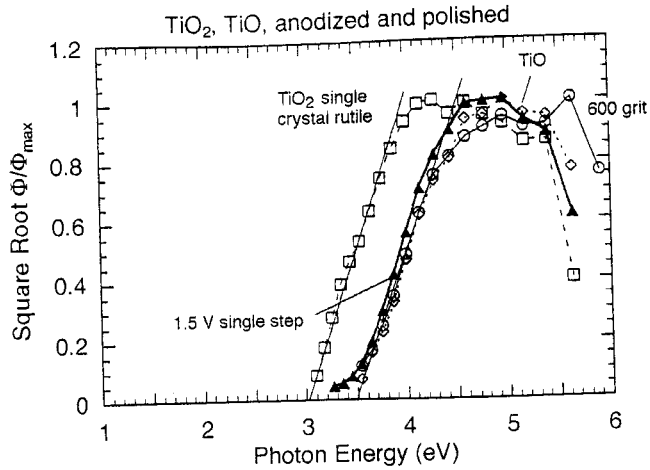

FIGURE 4. *The photospectra for 600-grit polished titanium, cubic TiO, and the acid-etched titanium (not shown) are all similar, with an indirect bandgap, E_{gap} = 3.5 eV. The 1.5-V single step anodized sample has a bandgap of 3.48 eV. These are different from single crystal rutile.*

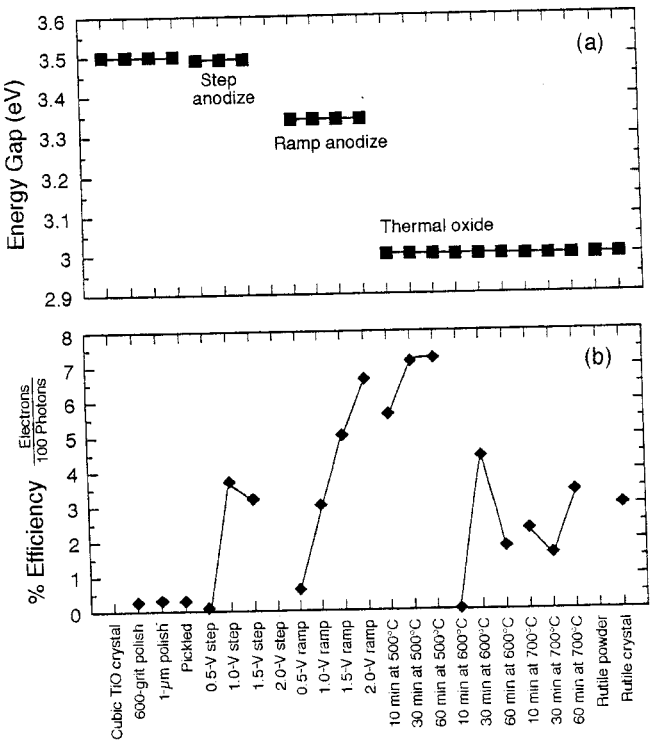

FIGURE 5. *Photoelectrochemical data is shown for the different surface treatments on titanium. Three distinct bandgaps are seen, with the % efficiency a function of thickness. (The bandgap of 3.2 eV for anatase is not shown.)*

ited a bandgap of 3.5 eV, which is 0.5 eV higher than the TiO_2 rutile (included for comparison). Cubic TiO is not a semiconductor, but rather a conductor,[36] so it cannot sustain the internal electric field necessary to create the photocurrent (Figure 1). Therefore, there must be another oxide or hydroxide of titanium on the cubic TiO surface that has the 3.5-eV bandgap.

Similar PEC measurements were carried out on the other surface finishes of titanium. A summary of the % efficiency (maximum Φ) and the extrapolated bandgaps are shown in Figures 5(a) and (b). Figure 5(a) shows a distinct clustering of the bandgaps. The thermal oxides all correspond to TiO_2 rutile with a bandgap of 3.0 eV. When randomly oriented rutile powder was PEC tested as described earlier, it also had a bandgap of 3.0 eV. The polished or pickled titanium surfaces had a bandgap of 3.5 eV, which was the same as that found on cubic TiO. This 3.5-eV bandgap is hypothesized to originate from an amorphous titanium oxide-hydroxide layer. In Figure 5(b), it appears that the efficiency increased as the oxide layer grew thicker, and then decreased after an optimum thickness was passed. (The 800°C sample was tested but the data is not included because the unusual photosignal had positive photocurrents at low energy and negative photocurrents at high energy, possibly occurring because of the formation of titanium nitrides and suboxides). The ramp anodized oxides had a bandgap of 3.35 eV, which was lower than the step-anodized oxides that were 3.48 eV. This effect of the anodizing rate has been reported by previous researchers.[30-32] The 3.35-eV bandgap is hypothesized to originate from a second amorphous titanium oxide-hydroxide layer.

Oxide films also were analyzed using EIS, and the curves for the 30-min thermally oxidized samples are shown in Figure 6. The higher temperature resulted in thicker oxides until 800°C (not shown) where the thermal oxide began spalling or cracking. The thickness of the oxides was calculated from impedance in the linear slope region of the EIS curves using Equation (2), and the combined data is

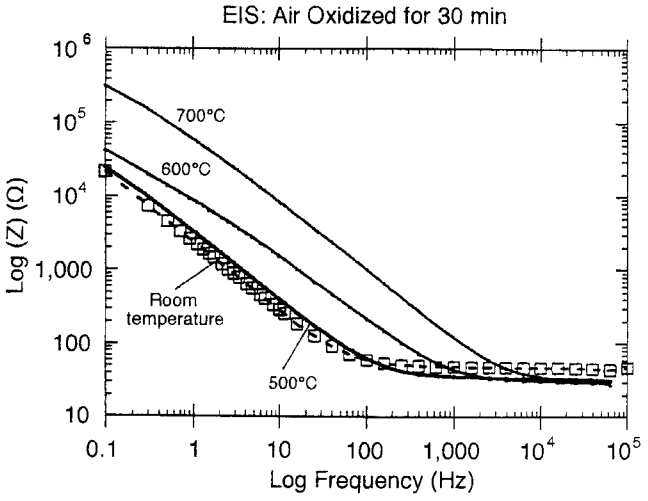

FIGURE 6. *EIS spectra for the titanium thermally oxidized for 30 min at various temperatures shows that 700°C has the highest impedance.*

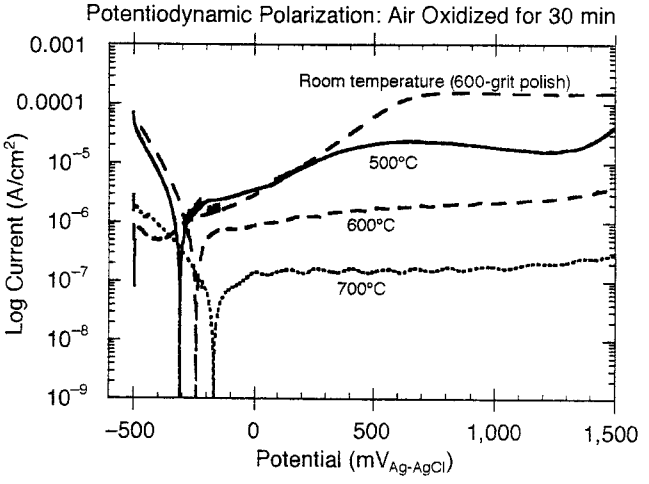

FIGURE 8. *PDP of thermal oxides show that the 30 min at 700°C had the lowest passive current in the synthetic seawater.*

shown in Figure 7. Thermal oxides on the right-hand side are rutile, and the value of $\varepsilon_1 = 110$ was used for the dielectric constant. Oxides on the left were not rutile, so a dielectric constant of $\varepsilon_1 = 48$ (the dielectric constant of anatase[3]) was used as a best approximation.

The PDP curves for the thermally oxidized samples are shown in Figure 8. The higher temperature oxides show a progressively lower passive current density and a higher corrosion potential (E_{corr}), which implies that the films are more protective and inert. The oxide formed at 700°C for 30 min shows the highest E_{corr} and the lowest passive current. Results for all the oxides measured are shown in Figures 9(a) and (b). Both anodizing and thermal oxidizing provide a thicker and more corro-

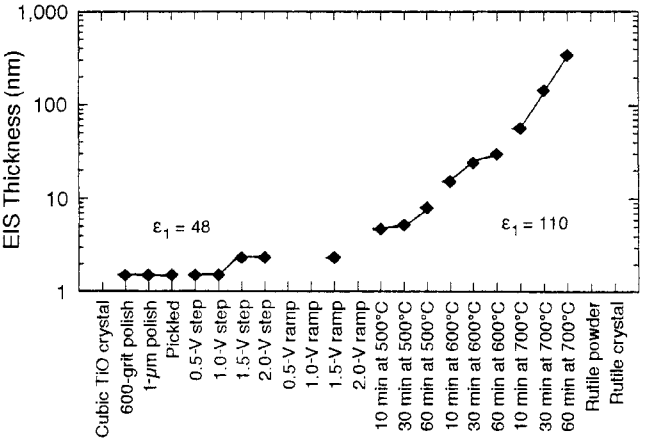

FIGURE 7. *The thickness of the oxides as measured via EIS and Equation (2). The dielectric constant was estimated as $\varepsilon_1 = 48$ (for anatase) or $\varepsilon_1 = 110$ (for rutile).*

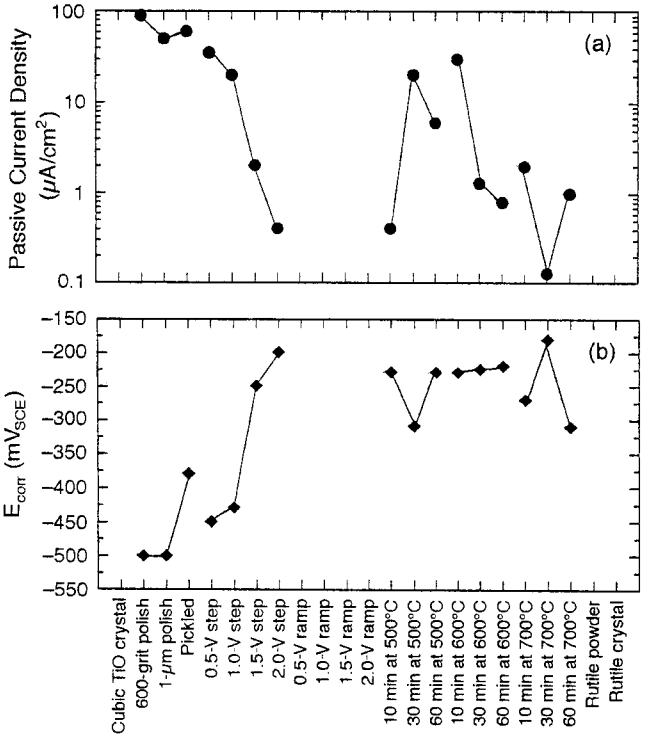

FIGURE 9. *Summary of the PDP data for the different surface treatments. The lower passive current corresponded to the more noble E_{corr}.*

sion-resistant film, as seen by the decrease in the passive current, and the increase in the E_{corr}.

GAXRD results are shown in Figures 10 and 11. Figure 10 shows the GAXRD results for the 600°C thermally oxidized sample, which demonstrates multiple TiO_2 rutile peaks and four peaks for titanium. The GAXRD for the 600-grit polished titanium surface in Figure 11 shows only titanium peaks and a small peak at 1.541Å, which corresponds to the

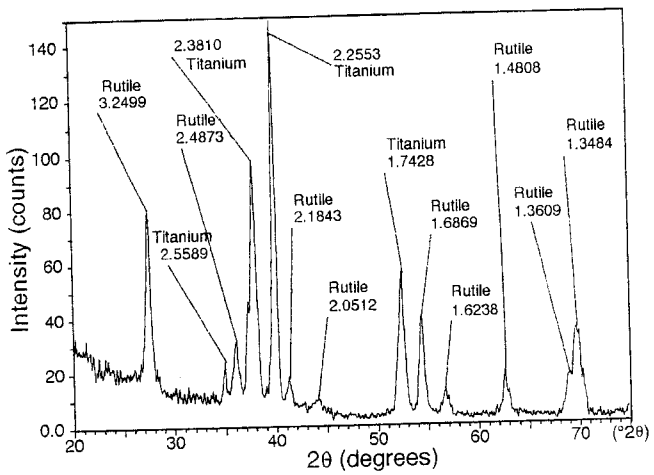

FIGURE 10. *GAXRD results for the 60 min at 600° C oxidized titanium showed rutile and titanium peaks.*

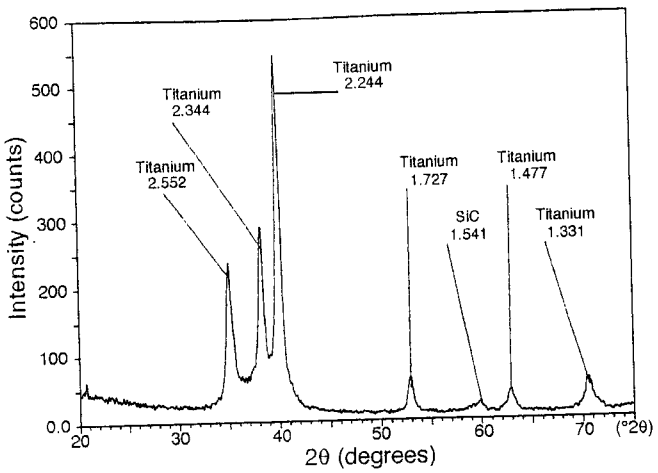

FIGURE 11. *GAXRD results for the 600-grit polished titanium showed only titanium peaks, with a small peak from the SiC polishing grit.*

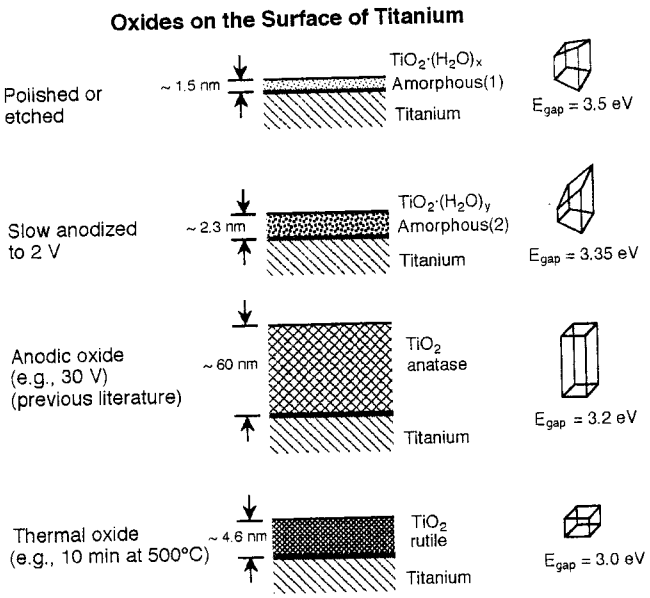

FIGURE 12. *The surface treatment determined the structure of titanium oxide that formed on the surface of titanium. (The gray band between the oxide layer and the titanium base metal denotes the titanium suboxides.)*

SiC used to polish the sample. There are no peaks for the oxide, so it is assumed to be either amorphous or too thin to measure.

Figure 12 is the summary of this paper combined with the previous literature. The surface oxide on titanium was highly dependent on the surface treatment. Polished or etched titanium had an amorphous(1) layer, with a bandgap of 3.5 eV. The ramp or slow anodized titanium had an amorphous(2) layer, with a bandgap of 3.35 eV. The titanium anodized > 50 V had an anatase crystal structure (based on the literature since tests were not duplicated here). Thermally anodized titanium had a TiO_2 rutile structure with a bandgap of 3.0 eV. (The gray band between the oxide layer and titanium base metal denotes titanium suboxides.) The most passive oxide was found on the air-oxidized titanium at 700°C for 30 min. EIS results illustrated that this thermal oxide offered thickness (high impedance in the sloped region) and minimal current leakage (high impedance at the low-frequency end).

CONCLUSIONS

- An amorphous(1) oxide (E_{gap} = 3.5 eV) was present on the surface of polished, pickled, and step-anodized titanium. A second amorphous(2) oxide (E_{gap} = 3.35 eV) was present on the surface of slow ramp-anodized titanium (to 2.0 V). TiO_2 rutile (E_{gap} = 3.0 eV) was present on the thermally oxidized titanium (500°C to 700°C).
- The optimum surface oxide for passivity and photocurrent generation was TiO_2 rutile grown by thermal oxidation in air. The TiO_2 rutile is denser, has a lower bandgap, and has a higher quantum yield than TiO_2 anatase.
- The n-type thermal oxide present on titanium heated between 500°C and 700°C in air was TiO_2 rutile with an indirect bandgap energy of 3.0 eV, which is the same as randomly oriented powder rutile or single crystal rutile. The highest quantum efficiency, 7% at 290 nm (4.3 eV), was found for the rutile thermal oxide (air oxidized at 500°C for 30 min to 60 min).
- The PDP and EIS tests showed that the thermally oxidized titanium has corrosion resistance superior to that of the pickled, polished, and anodized treatments. The TiO_2 rutile oxide formed at 700°C for 30 min showed the lowest passive current and the most noble E_{corr}. The thermal oxides formed at higher

temperatures and longer times showed a decrease in corrosion resistance as a result of thermal cracking and flaking of the thick oxide.

ACKNOWLEDGMENTS

The authors thank J.A. Mountford, Jr., of Timet for donating the titanium metal, M. Renavikar for his technical expertise, G. McManus and J.R. Blachere for their help with GAXRD, B. Evans for his help with the thermal oxidation, and D. Waldeck for the donation of the TiO_2 single crystals.

REFERENCES

1. M. Pourbaix, Atlas of Electrochemical Equilibria in Aqueous Solutions (Houston, TX: NACE International, 1974), p. 217.
2. J.L. Murray, Bull. Alloy Phase Diagr. 8, 2 (1987): p. 148-165.
3. R.J.H. Clark, "Titanium," in Comprehensive Inorganic Chemistry, ed. A.F. Trotman-Dickenson (Oxford, U.K.: Pergamon Press Ltd., 1973), p. 375-377.
4. V.V. Andreeva, Corrosion 20, 2 (1964): p. 35t-46t.
5. N.D. Tomashov, Corrosion and Protection of Metal Structural Materials (Moskva, USSR: English Translation of Korroziya Zashchita Konstruktsionnykh Metallischeskikh Materialov, 1961), p. 5-260.
6. J.S.L. Leach, D.H. Sidgwick, Proc. 8th Int. Cong. Metallic Corrosion (Frankfurt, Germany: Dechema, 1981), p. 82-86.
7. G. Blondeau, M. Froelicher, M. Froment, A. Hugot-Le Goff, J. Microsc. Spectrosc. Electron. 2 (1977): p. 27-38.
8. J. Yahalom, J. Zahavi, Electrochim. Acta 15 (1970): p. 1,429-1,435.
9. J.F. McAleer, L.M. Peter, J. Electrochem. Soc. 129 (1982): p. 1,252-1,260.
10. A.R. Prusi, Lj.D. Arsov, Corros. Sci. 33, 1 (1992): p. 153-164.
11. R.W. Schutz, L.C. Covington, Corrosion 37, 10 (1981): p. 585-591.
12. CODEWELD'-Titanium Tubing, TIMET Brochure (Denver, Colorado: Timet, 1996), p. 11-12.
13. T. Ohtsuka, M. Masuda, N. Sato, J. Electrochem. Soc. 132, 4 (1985): p. 787-792.
14. T. Shibata, Y.C. Zhu, Corros. Sci. 37, 2 (1995): p. 253-270.
15. J.C. Pesant, P. Vennereau, J. Anal. Chem. 106 (1980): p. 103-113.
16. F.P. Koffyberg, K. Dwight, A. Wold, Solid State Commun. 30 (1979): p. 433-437.
17. J.W. Schultze, U. Stimming, J. Weise, Ber. Bunsenges. Phys. Chem. 86 (1982): p. 276-282.
18. K. Leitner, J.W. Shultze, U. Stimming, J. Electrochem. Soc. 133, 8 (1986): p. 1,561-1,568.
19. P.S. Tyler, M.R. Kozlowski, W.H. Smyrl, J. Electroanal. Chem. 237 (1987): p. 295-302.
20. T.D. Burleigh, Corrosion 45, 6 (1989): p. 464-472.
21. M.R. Kozlowski, P.S. Tyler, W.H. Smyrl, R.T. Atanasoski, Surf. Sci. 194 (1988): p. 505-530.
22. J.W. Halley, M. Kozlowski, M. Michalewicz, W. Smyrl, N. Tit, Surf. Sci. 256 (1991): p. 397-408.
23. I.D. Makuta, S.K. Poznyak, A.I. Kulak, Electrochim. Acta 40, 11 (1993): p. 1,761-1,767.
24. L. Kavan, M. Gratzel, S.E. Gilbert, C. Klemenz, H.J. Scheel, J. Am. Chem. Soc. 118 (1996): p. 6,716-6,723.
25. J. Marsh, D. Gorse, Electrochim. Acta 43, 7 (1998): p. 659-670.
26. A. Michaelis, J.W. Schultze, Thin Solid Films 274 (1996): p. 82-94.
27. J.W. Schultz, S. Kudelka, The Electrochemical Society Interface (1997): p. 28-31.
28. S. Kudelka, J.W. Schultze, Electrochim. Acta 42, 18 (1997): p. 2,817-2,825.
29. M. Schweinsberg, S. Kudelka, A. Michaelis, J.W. Schultze, Mater. Corros. 49 (1998): p. 161-168.
30. A. Goosens, Surf. Sci. 371 (1997): p. 390-398.
31. D.J. Blackwood, L.M. Peter, Electrochim. Acta 34, 11 (1989): p. 1,505-1,511.
32. J.-L. Delplancke, A. Garnier, Y. Massiani, R. Winand, Electrochim. Acta 39, 8/9 (1994): p. 1,281-1,289.
33. P. Schmuki, M. Buchler, S. Virtanen, H. Böhni, R. Mueller, L.J. Gauckler, J. Electrochem. Soc. 142, 10 (1995): p. 3,336-3,342.
34. T.D. Burleigh, A.T. Smith, J. Electrochem. Soc. 138, 8 (1991): p. L34-35.
35. "Powder Diffraction File," Joint Committee on Powder Diffraction Standards (JCPDS), (Philadelphia, PA: 1971-1977).
36. J.M. Honig, Electrodes of Conductive Metallic Oxides, ed. S. Trasatti (Amsterdam, The Netherlands: Elsevier Scientific Publishers, 1980), p. 2-96.